Parametrized modified gravity and the CMB bispectrum

PHYSICAL REVIEW D **86,** 063517 (2012)

Parametrized modified gravity and the CMB bispectrum

Eleonora Di Valentino,[1] Alessandro Melchiorri,[1] Valentina Salvatelli,[1] and Alessandra Silvestri[2]
[1]*Physics Department and INFN, Università di Roma "La Sapienza", Ple Aldo Moro 2, 00185 Rome, Italy*
[2]*Department of Physics, MIT, Cambridge, Massachusetts 02139, USA*
(Received 27 April 2012; published 19 September 2012)

We forecast the constraints on modified theories of gravity from the cosmic microwave background (CMB) anisotropies bispectrum that arises from correlations between lensing and the Integrated Sachs-Wolfe effect. In models of modified gravity the evolution of the metric potentials is generally altered and the contribution to the CMB bispectrum signal can differ significantly from the one expected in the standard cosmological model. We adopt a parametrized approach and focus on three different classes of models: Linder's growth index, Chameleon-type models, and $f(R)$ theories. We show that the constraints on the parameters of the models will significantly improve with future CMB bispectrum measurements.

DOI: 10.1103/PhysRevD.86.063517 PACS numbers: 98.80.Es, 95.30.Sf, 98.80.Jk

I. INTRODUCTION

Cosmic acceleration is one of the major challenges faced by modern cosmology and understanding the very nature of what is sourcing it is the main focus of upcoming and future cosmological experiments. Several approaches to the phenomenon of cosmic acceleration have been proposed in the literature, including modifications of the laws of gravity on large scales in order to allow for self-accelerating solutions in matter-only universes. Well-known examples of modified theories of gravity are $f(R)$ models [1–5], or the more general scalar–tensor theories [6–9], the Dvali-Gabadadze-Porrati (DGP) model [10,11], and its further extensions such as degravitation [12]. In the past years several authors have analyzed constraints on modified gravity, or more generally departures from the cosmological standard model, both using current data sets as well as doing forecasts for future surveys [13–28] In this paper we focus on certain classes of modified gravity and adopt a parametrized approach to forecast the constraints achievable from measurements of the CMB bispectrum from future experiments.

Future high-resolution CMB maps will have the ability of detecting higher-order correlations in the temperature distribution at high significance (see e.g., Ref. [29] and references therein). While the CMB anisotropy distribution is generally expected to be Gaussian to high accuracy, small non-Gaussianities could be produced in the early universe, during inflation (commonly referred to as primordial non-Gaussianities, see e.g., [30]) as well as be sourced, at a much later epoch, by the interaction of CMB photons with the local universe. For instance, the lensing of CMB photons by dark matter structure produces a clear non-Gaussian signal in the CMB trispectrum (the Fourier transform of the four-point correlation function), which can be used to constrain the amplitude of the lensing potential. Such a signal, already discovered by the recent ACT [31] and SPT [32] experiments, helps in further constraining cosmological models.

In this paper we study the implications of another non-Gaussian signal expected in the CMB, i.e., the one arising from cross-correlations between lensing and the Integrated Sachs-Wolfe effect (ISW), which affects the CMB bispectrum, i.e., the three-point correlation function.

The signature of the lensing-ISW (L-ISW hereafter) correlations in the CMB bispectrum has already been discussed by several authors (see e.g., Refs. [33–43]) Assuming the standard cosmological scenario, ΛCDM, the L-ISW bispectrum should be detected at the significance level of 4–5 standard deviations. In Refs. [35,37,38] the possibility of constraining cosmological parameters through this detection has been considered; in particular, it has been shown that an accurate measurement of the L-ISW will help in constraining the equation of state and the fractional density of dark energy. Here we shall analyze the potential of the L-ISW signal to constrain modified theories of gravity. In the latter, the evolution of the metric potentials can generally differ significantly from the ΛCDM prediction, therefore it is natural to expect that the L-ISW bispectrum would provide valuable constraints on these theories.

The paper is organized as follows. In Sec. II we present the set of modified gravity models considered for our analysis and in Sec. III we review the L-ISW bispectrum. In Sec. IV we describe the analysis method and in Sec. V we present our results. We conclude in Sec. VII.

II. PARAMETRIZED MODIFIED GRAVITY

Many models of modified gravity have been proposed as alternatives to ΛCDM, and analysing them one by one is impractical. The idea behind parametrized versions of modified gravity is exactly that of encompassing several models into a single framework. The parametrizations that we consider for our analysis cover a fairly large sample of theories and allow us to draw quite general conclusions about the constraining power of the data considered.

In our analysis we fix the background to that of the ΛCDM model of cosmology. The latter is currently in very good agreement with all observables constraining the expansion history, and many models of modified gravity can mimic it while introducing significant modifications at the level of perturbations. Therefore, fixing the background to ΛCDM, allows us to isolate the effects of departures at the level of growth of structure, where we expect the most significant deviations.

A. Linder model

In Ref. [44] Linder introduced a simple parametrization of the growth of density perturbations in the linear regime, via a single parameter, the growth index γ (which we will denote with γ_L), defined through

$$g(a) = e^{\int_0^a d\ln a[\Omega_m(a)^{\gamma_L} - 1]}. \quad (1)$$

The idea is that of capturing independently the information from the expansion and the growth history, respectively, in Ω_m and γ_L. Since in our analysis we fix the background to ΛCDM, $\Omega_m(a)$ is determined by that and the only parameter of interest will be γ_L.

In the cosmological concordance model, ΛCDM, as well as in vanilla-type dark energy models, γ_L is to good approximation constant and equal to $\gamma_L \approx 6/11$. While it can generally be a function of time and scale, in several models of modified gravity it can still be approximated by a number, which often differs significantly from the ΛCDM value. For instance in the braneworld gravity of the DGP model, $\gamma_L \approx 0.68$ to good approximation over the whole history [44]. Things are more complicated for scalar-tensor models where often the time- and scale-dependence of γ_L cannot be neglected. However, γ_L remains a powerful *trigger* parameter, since any deviation of it from $\approx 6/11$ would indicate a breakdown of the cosmological concordance model.

As a starting point for our analysis, we assume $\gamma_L \approx$ const. and forecast constraints on this simple one parameter model.

B. Chameleon-type models

Chameleon-type theories correspond to gravity plus a scalar degree of freedom which is conformally coupled to matter fields, and has therefore a profile and a mass which depend on the local density of matter. The common action for such theories is

$$S = \int d^4x\sqrt{-g}\left[\frac{M_P^2}{2}R - \frac{1}{2}g^{\mu\nu}(\nabla_\mu\phi)(\nabla_\nu\phi) - V(\phi)\right] + S_i(\chi_i, e^{-\alpha_i(\phi)/M_P}g_{\mu\nu}), \quad (2)$$

where ϕ is the scalar d.o.f., χ_i is the i th matter field, and $\alpha_i(\phi)$ is the coupling of χ_i to ϕ. We will limit ourselves to cases in which the coupling is a linear function of the scalar field, i.e., $\alpha_i(\phi) \propto \beta_i\phi$. A well-known example of the latter are $f(R)$ theories as we discuss in Sec. II C.

The free parameters of these theories are the mass scale of the scalar field and the couplings β_i. Since we consider constraints from late-time cosmology, we are interested only in the coupling to dark matter, and therefore drop the index i.

While the modifications enter through the coupling of the scalar field to matter, and therefore change the energy-momentum conservation equations, it is possible to keep the latter unchanged and effectively absorb the modifications of the evolution of perturbations in the Poisson and anisotropy equations. The latter are commonly parametrized with two functions μ and γ, as follows:

$$k^2\Psi = -\frac{a^2}{2M_P^2}\mu(a,k)\rho\Delta, \quad (3)$$

$$\frac{\Phi}{\Psi} = \gamma(a,k), \quad (4)$$

where $\rho\Delta \equiv \rho\delta + 3\frac{aH}{k}(\rho + P)v$ is the comoving density perturbation and Φ and Ψ are the scalar metric perturbations in conformal Newtonian gauge (with the convention $\delta g_{00} = -2a^2\Psi$ and $\delta g_{ij} = -2a^2\Phi\delta_{ij}$). Furthermore, for Chameleon-type theories μ and γ are well represented by the parametrization introduced in Ref. [45]

$$\mu(a,k) = \frac{1 + \beta_1\lambda_1^2k^2a^s}{1 + \lambda_1^2k^2a^s}, \qquad \gamma(a,k) = \frac{1 + \beta_2\lambda_2^2k^2a^s}{1 + \lambda_2^2k^2a^s}, \quad (5)$$

where the parameters β_i can be thought of as dimensionless couplings, λ_i as dimensional length-scales, and s is determined by the time evolution of the characteristic length-scale of the theory, i.e., the mass of the scalar d.o.f. As shown in Ref. [17], in the case of Chameleon-type theories the parameters $\{\beta_i, \lambda_i^2\}$ are related in the following way:

$$\beta_1 = \frac{\lambda_2^2}{\lambda_1^2} = 2 - \beta_2\frac{\lambda_2^2}{\lambda_1^2} \quad (6)$$

and $1 \lesssim s \lesssim 4$, so that effectively the degrees of freedom are one coupling and a time-evolving length scale.

C. $f(R)$ theories

As it becomes clear in the Einstein frame, $f(R)$ theories are a subclass of the models described by action (2), corresponding to a universal fixed coupling $\alpha_i = \sqrt{2/3}\phi$. Therefore they can also be described by the parametrization in (5). It can be easily seen that the fixed coupling $\alpha_i = \sqrt{2/3}\phi$ gives $\beta_1 = 4/3$ and $\beta_2 = 1/2$. Furthermore, viable $f(R)$ models that closely mimic ΛCDM have $s \sim 4$ [17]; therefore, using (6), the number of free parameters in Eqs. (5) can be effectively reduced to one length scale, e.g., the length scale λ_1.

The latter is directly related to the mass scale of the scalar degree of freedom introduced by these theories and represented by $f_R \equiv df/dR$, known as the *scalaron*. Specifically, λ_1 sets the inverse mass scale of the scalaron today, i.e., $\lambda_1 = 1/m^0_{f_R}$. The results in the literature are usually presented in terms of a parameter B_0 which is related to λ_1 as follows [46]:

$$B_0 = \frac{2H_0^2\lambda_1^2}{c^2}. \tag{7}$$

Studying this particular subclass is interesting because some models belonging to this category have been shown to be cosmologically viable and pass local tests of gravity [47].

III. THE LENSING-ISW BISPECTRUM

As it is well known, if the expansion of the Universe is not matter-dominated (i.e., $\Omega_m \neq 1$), the time variation of the gravitational potential provides an additional source of CMB anisotropies; restricting to the linear regime, this effect is known as the Integrated Sachs Wolfe (ISW) effect [48], given by

$$\frac{\delta T}{T}(\mathbf{n})|_{ISW} = \int d\tau(\dot{\Psi}[(\tau_0 - \tau)\mathbf{n}, \tau] + \dot{\Phi}[(\tau_0 - \tau)\mathbf{n}, \tau]), \tag{8}$$

where $\mathbf{n}$ is a direction in the sky, τ is conformal time, τ_0 is the time today, and the dot denotes differentiation with respect to τ. This adds a secondary anisotropy to the primordial signal and a significant contribution from it is expected at late times, when the Universe starts accelerating.

Furthermore, the weak gravitational lensing by matter density fluctuations between us and the last scattering surface shifts the observed direction of photons. In practice, the temperature anisotropy measured by an observer in the direction $\mathbf{n}$ is actually the anisotropy in the direction $(\mathbf{n} + \nabla\phi(\mathbf{n}))$, i.e.,

$$\delta\tilde{T}(\mathbf{n}) = \delta T(\mathbf{n} + \nabla\phi(\mathbf{n})), \tag{9}$$

where $\delta\tilde{T}(\mathbf{n})$ is the lensed anisotropy and $\delta T(\mathbf{n})$ is the unlensed one (primordial plus ISW). The deflection angle is written in terms of the *lensing potential* ϕ, which is a weighted integral of the Weyl potential $\Phi + \Psi$ over the line of sight:

$$\phi(\mathbf{n}) = \int_0^{\chi_*} d\chi g(\chi)[(\Psi + \Phi)(\mathbf{n}, \chi)]. \tag{10}$$

Here χ is the comoving distance from the observer and $g(\chi) = (\chi_* - \chi)/(\chi\chi_*)$ with χ_* the distance at the last scattering surface.

The Weyl potential enters both in the ISW and the lensing kernel, therefore the two effects are correlated and they contribute a nonzero third-order statistic in the CMB, i.e., the L-ISW bispectrum. As usual, it is convenient to consider an expansion in spherical harmonics of the temperature field:

$$\frac{\delta T}{T}(\mathbf{n}) = \sum_{\ell=2}^{\infty}\sum_{m=-\ell}^{\ell} a_{\ell m}Y_{\ell m}(\mathbf{n}) \tag{11}$$

as well as of the lensing potential, $\phi(\mathbf{n}) = \sum_{\ell,m}\phi_{\ell m}Y_{\ell m}(\mathbf{n})$. By Taylor-expanding Eq. (9) in the lensing potential, and applying the above harmonic expansions, one obtains the following relation between the lensed and unlensed multipole coefficients, (to first order in the lensing multipoles):

$$\tilde{a}_{\ell_1 m_1} \approx a_{\ell_1 m_1} + \sum_{\ell_2 m_2 \ell m} f_{\ell_1\ell_2\ell}a^*_{\ell_2 m_2}\phi^*_{\ell m}\begin{pmatrix} \ell_1 & \ell_2 & \ell \\ m_1 & m_2 & m \end{pmatrix}, \tag{12}$$

where the coefficient $f_{\ell_1\ell_2\ell}$ is given by

$$f_{\ell_1\ell_2\ell} = \left(\frac{-\ell_1(\ell_1+1) + \ell_2(\ell_2+1) + \ell(\ell+1)}{2}\right)\Upsilon_{\ell_1\ell_2\ell}, \tag{13}$$

with

$$\Upsilon_{\ell_1\ell_2\ell_3} \equiv \sqrt{\frac{(2\ell_1+1)(2\ell_2+1)(2\ell_3+1)}{4\pi}}\begin{pmatrix} \ell_1 & \ell_2 & \ell_3 \\ 0 & 0 & 0 \end{pmatrix}. \tag{14}$$

Then, the angle-averaged CMB bispectrum generated by the lensing-ISW correlation is given by

$$\begin{aligned} B_{\ell_1\ell_2\ell_3} &= \sum_{m_1 m_2 m_3}\begin{pmatrix} \ell_1 & \ell_2 & \ell_3 \\ m_1 & m_2 & m_3 \end{pmatrix}\langle\tilde{a}_{\ell_1 m_1}\tilde{a}_{\ell_2 m_2}\tilde{a}_{\ell_3 m_3}\rangle \\ &= f_{\ell_1\ell_2\ell_3}C^{T\phi}_{\ell_2}C^{TT}_{\ell_3} + 5\,\text{perm}\ldots, \end{aligned} \tag{15}$$

where C^{TT}_ℓ is the temperature (primordial plus ISW) power spectrum and $C^{T\phi}_\ell$ is the cross temperature-lensing angular power spectrum, $C^{T\phi}_\ell = \langle\phi^*_{\ell m}a_{\ell m}\rangle$, which depends on the Weyl potential and its first time-derivative (see e.g., Ref. [35]). In deriving (15) we have implicitly assumed the statistical isotropy of the Universe and have averaged the three-point correlation function (in harmonic space) over the orientation of triangles by mean of rotational invariance. Numerical codes evolving perturbations typically work with the reduced bispectrum, defined via

$$B_{\ell_1\ell_2\ell_3} = \Upsilon_{\ell_1\ell_2\ell_3}b_{\ell_1\ell_2\ell_3}. \tag{16}$$

In Fig. 1 we plot different theoretical predictions for $C^{T\phi}_\ell$ and the reduced bispectrum $b_{\ell_1\ell_2\ell_3}$ computed with the publicly available code MGCAMB [49]. As can be seen, the L-ISW bispectrum is clearly sensitive to modifications of gravity and in principle can be used to put constraints on models of modified gravity. In the next section we describe the analysis method that we have used to forecast the latter for Planck-like experiments.

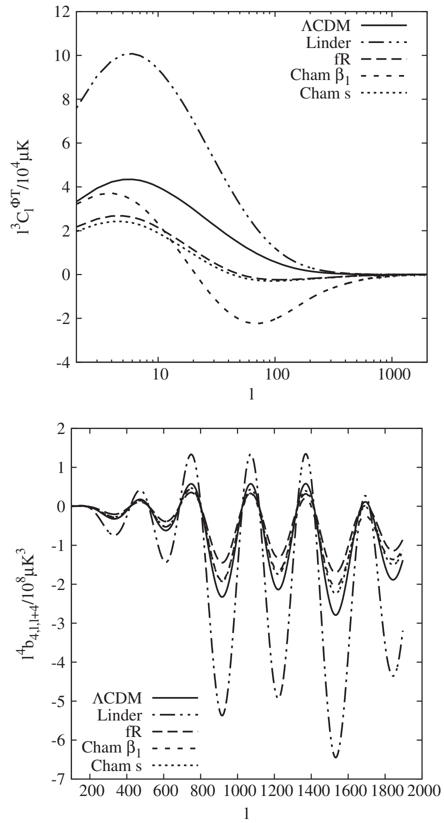

FIG. 1. Dependence of the cross temperature-lensing $C_\ell^{T\phi}$ angular spectra (top panel) and of the reduced bispectrum (bottom panel) on modified gravity parameters for the different models considered in the analysis. The solid curves correspond to ΛCDM, the dotted and dashed curves to the Linder parametrisation with $\gamma_L = 0.645$, the long-dashed curves to an f(R) model with $B_0 = 0.42$, the short-dashed curves to a Chameleon model (Cham β_1) with $\beta_1 = 1.3$, $B_0 = 0.50$ $s = 2.0$, and the dotted line to a Chameleon model (Cham s) with $\beta_1 = 1.3$, $B_0 = 0.50$, $s = 3.3$.

IV. FUTURE CONSTRAINTS FROM CMB: METHOD

We shall estimate the potential of upcoming L-ISW bispectrum measurements from CMB Planck-like experiments to constrain the modified gravity theories described in the previous section. We perform a likelihood analysis from the power spectrum, L-ISW bispectrum and their combination in order to compare the parametrized models of Sec. II to a fiducial model, chosen to reproduce a ΛCDM cosmology. We fix the cosmological parameters according to the WMAP 7-year data best fit [50] and vary only the parameters entering the parametrizations described in Sec. II. Spanning over the parameter space, we calculate the power spectrum and L-ISW bispectrum using MGCAMB and build the likelihoods as described in the following.

Each theoretical model is then compared to the fiducial model with a simple χ^2 function which assumes that the power spectrum and bispectrum can be safely described as Gaussian variables [35,38]. For the standard C_ℓ^{TT} temperature anisotropy power spectrum we have

$$\chi_s^2 = \sum_\ell^{1000}\left[\frac{C_\ell^{TT,th} - C_\ell^{TT,fid}}{\sigma_\ell^s}\right]^2, \tag{17}$$

where the uncertainty σ^s is given by

$$\sigma_\ell^s = \sqrt{\frac{2}{(2\ell+1)}}C_\ell^{TT}, \tag{18}$$

We do not include any covariance noise matrix in Eq. (18), effectively assuming σ^s to be cosmic-variance limited up to $\ell = 1000$, which is a good approximation for future Planck-like experiments.

For the bispectrum we have

$$\chi_b^2 = \sum_{\ell_1,\ell_2,\ell_3=2}^{l_{\max}}\left[\frac{B^{\rm th}_{\ell_1\ell_2\ell_3} - B^{fid}_{\ell_1\ell_2\ell_3}}{\sigma^b_{\ell_1\ell_2\ell_3}}\right]^2, \tag{19}$$

where the sum is over all possible combinations of ℓ_1, ℓ_2, ℓ_3 with ($\ell_1 \le \ell_2 \le \ell_3$), $\ell_1 + \ell_2 + \ell_3$ even and we set $\ell_{\rm max} = 1000$, which roughly corresponds to the maximum multipole for which the experimental noise of a Planck-like experiment is fully dominated by cosmic variance (since at higher multipoles the contamination from foreground point sources starts to be relevant).

The uncertainty $\sigma^b_{\ell_1\ell_2\ell_3}$ is given by

$$(\sigma^b_{\ell_1\ell_2\ell_3})^2 = n_{\ell_1\ell_2\ell_3}C^{TT}_{\ell_1}C^{TT}_{\ell_2}C^{TT}_{\ell_3}, \tag{20}$$

where $n_{\ell_1\ell_2\ell_3}$ is 6 for equilateral configurations ($\ell_1 = \ell_2 = \ell_3$), 2 for isoscele ones (with two multipoles equal), and 1 for the scalene ones (when all the multipoles are different). There is no noise covariance matrix in the C_ℓ^{TT}. In the analysis we assume a sky coverage of $f_{\rm sky} = 0.65$. This very conservative assumption increases the above variances by a term $1/f_{\rm sky}$.

Once the χ^2 functions are computed, we can build the separate likelihoods for the power spectrum and bispectrum data, respectively:

$$\mathcal{L}_{s,b} = \exp\left(-\frac{\chi^2_{s,b}}{2}\right). \tag{21}$$

Neglecting the correlation between power spectrum and bispectrum, we can further combine them in a total likelihood as follows:

$$\mathcal{L}_c = \mathcal{L}_s\mathcal{L}_b = \exp\left(-\frac{\chi_b^2 + \chi_s^2}{2}\right). \tag{22}$$

In the calculation of the likelihood from the CMB angular power spectrum we do not include the lensing term that is clearly correlated with L-ISW bispectrum. Furthermore, when combining the two likelihoods like in (22), we are neglecting correlations between power spectrum and bispectrum data that could arise from the large-scale ISW term. As we will see in the next section this is a good approximation since the bispectrum will constrain modified gravity parameters with a much stronger significance than power spectrum data alone. When computing the bispectrum we do not include the nonlinear Rees-Sciama term, since that would require a modeling of nonlinearities in modified gravity. The exclusion of the RS term is expected to affect our results at most by $\sim 17\%$, and therefore should not change our conclusions to a significant level. We plan to investigate in a future work the nonlinear RS term in the framework of modified gravity.

Finally, since we are modeling the (primordial plus ISW) power spectrum as a Gaussian variable, we are effectively neglecting any inflationary non-Gaussian signal; furthermore, we ignore contributions to the bispectrum from the lensing-Sunyaev-Zel'dovich correlation. Both signals could anyway be removed exploiting their different angular dependence (see e.g., Ref. [51]).

For each theoretical model of Sec. II, while keeping the cosmological parameters fixed to their WMAP 7-year values, we vary the modified gravity parameter(s) (one at a time for the models that have more than one parameter), and compute the power spectrum and the L-ISW reduced bispectrum with MGCAMB; we then use Eq. (16) to compute the L-ISW bispectrum from the reduced one. We also choose a fiducial model, as discussed in the following, and compute the corresponding power spectrum and bispectrum. Once a sufficient number of spectra is calculated, we compute the likelihood profiles and extract the confidence levels on the parameter of interest.

For each parametrization, we choose a fiducial model based on a set of parameters that are, for most of the cases, the parameters that would reduce the cosmology to the ΛCDM one. In the case of the Linder model this is achieved by setting $\gamma_L = 0.555$ [44]. For $f(R)$ theories, $B_0 = 0$ is the value giving $\mu = 1 = \gamma$, which are the values of these functions in ΛCDM. For chameleon theories the choice of the fiducial model is more complicated. Let us start employing the dimensionless parameter B_0 (7) in place of the length-scale λ_1, so that the parameters for these models become (B_0, s, β_1). As a matter of fact, we have three free parameters, no strong theoretical reasons to fix two of them, and a complete degeneracy among the parameters when trying to reproduce ΛCDM, i.e., if we fix either $B_0 = 0$ or $\beta_1 = 1$. We therefore proceed by making a somewhat arbitrary choice on the fiducial model, fixing $\beta_1 = 1$, $B_0 = 0.5$, and $s = 2$ when studying the forecasted constraints on β_1 and $\beta_1 = 1.3$, $B_0 = 0.5$, $s = 2$ when studying the forecasted constraints at varying s.

In the case of Linder's model we evaluate the likelihoods in the range $0.475 \leq \gamma_L \leq 0.635$, at steps of 0.002 for values near the fiducial one and at steps of 0.01 for values near the boundaries. In the case of $f(R)$ we explore the likelihood function in the range $0 \leq B_0 \leq 0.7$, varying B_0 at steps of 0.1. In the chameleon case we use a step of 0.01 for β_1 and of 0.2 for s.

TABLE I. Forecasted constraints on γ_L of Linder model from the power spectrum (**S**), bispectrum (**B**), and combined (**C**) analyses.

	Fiducial	**S** 95% c.l.	**B** 95% c.l.	**C** 95% c.l.
γ_L	0.555	$^{+0.044}_{-}$	$^{+0.060}_{-0.056}$	$^{+0.034}_{-0.042}$

V. RESULTS & CONSTRAINTS

A. Linder model

In Table I and Fig. 2 we report the forecasted constraints on γ_L from the power spectrum, the L-ISW bispectrum and the combined analyses. As we can see, the power spectrum and bispectrum data are somewhat complementary: the CMB bispectrum is more powerful in constraining the γ_L parameter in the region of values lower than those of the fiducial one; on the contrary, the temperature anisotropy spectrum is more efficient for larger values. The non-Gaussian shape of the likelihood from the temperature power spectrum can be easily understood by the fact that even in the case of a small ISW signal (when $\gamma_L \to 0$) the angular power spectrum is different from zero and still provides a reasonable fit to the data. The bispectrum is, on the contrary, not null only if the ISW is different from zero and it therefore provides a much more reliable way to detect it.

As we can see, power spectrum data provides solely an upper limit for γ_L, leaving it practically unconstrained on the lower tail. On the contrary, bispectrum data give a $\sim 5\%$ error on γ_L. When power spectrum and bispectrum data are combined there is a substantial improvement in the measurement.

B. Chameleon models

The forecasted constraints on Chameleon models from the power spectrum, L-ISW bispectrum, and combined analyses are reported in Table II and Fig. 3.

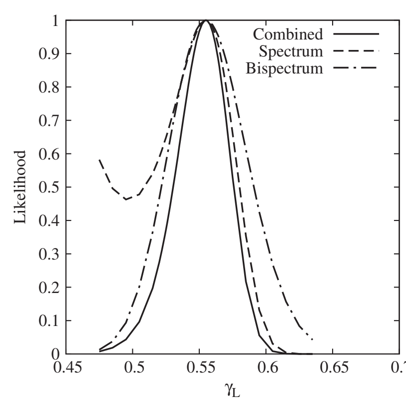

FIG. 2. Likelihood distribution function for the growth index γ_L (1) from the analysis of power spectrum, bispectrum, and combined data.

TABLE II. Forecasted constraints at 1 standard deviation on the Chameleon models parameters β_1 and s coming from the analysis of power spectrum (**S**), bispectrum (**B**), and combined (**C**) datasets.

	Fiducial	**S** 68% c.l.	**B** 68% c.l.	**C** 68% c.l.
β_1	1.00	$^{+0.25}_{-0.17}$	$^{+0.10}_{-0.13}$	$^{+0.09}_{-0.10}$
s	2.00	$^{+0.55}_{-0.17}$	$^{+0.42}_{-0.28}$	$^{+0.30}_{-0.15}$

As for the Linder model, the two data sets are complementary in constraining the Chameleon parameters. The simple temperature power spectrum is more powerful in constraining values of $\beta_1 \leq 0.75$, i.e., the lower tail, while the bispectrum data provide stronger constraints on the higher tail, where the power spectrum data leave the parameter practically unconstrained. The same behavior is seen for the likelihood distribution of the s parameter. Small values of s ($s < 2$) can be better constrained by temperature spectrum data. However, large values of s are left unconstrained from the temperature spectrum and, on the contrary, are significantly constrained when using the bispectrum. This is related, as we already explained when discussing constraints on γ_L, to the entity of the ISW signal in the two tails; namely, the power spectrum looses constraining power in the parameter range where the ISW is suppressed and tends to zero.

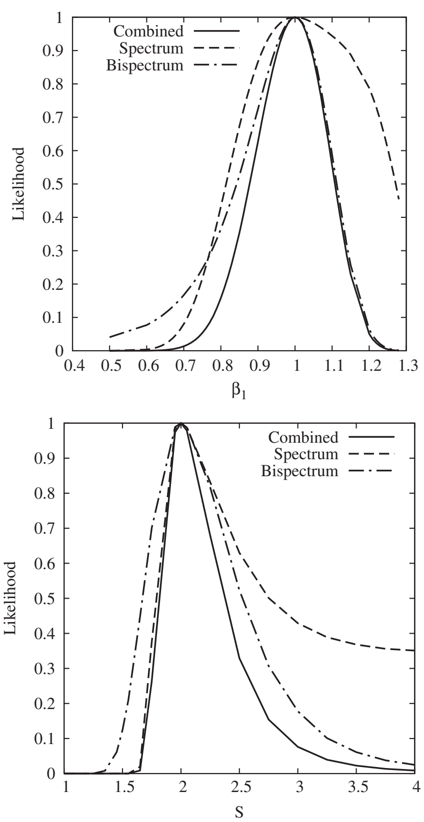

FIG. 3. Likelihood distribution function for Chameleon models from the power spectrum, bispectrum, and the combined analyses. The top panel gives the likelihood of the parameter β_1 when B_0 and s are fixed to $B_0 = 0.5$ $s = 2$; the bottom panel gives the likelihood for s when B_0 and β_1 are fixed to $B_0 = 0.5$ and $\beta_1 = 1.3$.

TABLE III. Forecasted constraints at 1 standard deviation on $f(R)$ theory parameter B_0 coming from the analysis of power spectrum (**S**), bispectrum (**B**), and combined (**C**) datasets.

	Fiducial	**S** 68% c.l.	**B** 68% c.l.	**C** 68% c.l.
B_0	0	<0.61	<0.14	<0.10

C. $f(R)$ theories

In Table III and Fig. 4 we report the forecasted constraints on $f(R)$ models from the power spectrum, L-ISW bispectrum and combined analyses. In this case, the constraints coming from the bispectrum are definitely tighter than the ones from the temperature spectrum. Once again, this is related to the ISW signal, which is suppressed with respect to ΛCDM one for all the values of B_0 in the range $0 < B_0 < 3/2$ (becoming null at $B_0 = 3/2$) [52]. Current constraints from ISW data from CMB-galaxy correlations are of the order of $B_0 < 0.4$ [26]. As we show, the L-ISW bispectrum can clearly improve CMB constraints on these theories, tightening the bounds by a factor of six.

VI. COMPARISON WITH CURRENT AND FUTURE BOUNDS ON MODIFIED GRAVITY

Let us compare our findings with the constraints (existing and forecasted) that can be found in the literature on the same models of modified gravity. In Refs. [26] the authors studied constraints on $f(R)$ models from a combination of current CMB ISW data and luminosity distances from Type Ia supernovae, obtaining the bound $B_0 < 0.4$ at 68% c.l. Comparing with our analysis, we can see that the bispectrum information considered in this paper is expected to give an improvement of a factor ~4. CMB weak lensing detections that will be performed by the Planck satellite experiment via

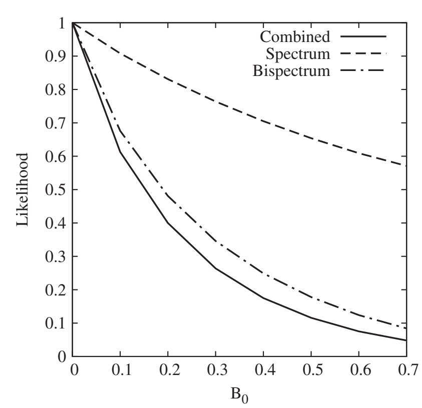

FIG. 4. Likelihood distribution function for the parameter B_0 describing $f(R)$ theories from the analysis of power spectrum, bispectrum, and combined data.

measurements of the CMB trispectrum are expected to bound B_0 to the ~ 0.01 level (see e.g., Refs. [27,53]), i.e., about one order of magnitude better than the bounds we forecast in this paper. An indication in the Planck bispectrum of ISW-Lensing non-Gaussianity should therefore produce a relevant signal in the trispectrum. Combining bispectrum and trispectrum analyses could therefore be very helpful in discriminating from a primordial, inflationary, signal. The further inclusion of weak lensing data as those expected from the Euclid satellite experiment will further constrain B_0 by one order of magnitude.

One advantage of the bispectrum data with respect to the ISW data from cross correlations of CMB maps with galaxy surveys will be the independence from the galaxy bias. As for the CMB trispectrum, it would certainly be useful to combine the data with that from the CMB bispectrum since the two data sets depend on different functions of the metric potentials; the bispectrum depends on the derivative of the potentials, while the lensing trispectrum only on their sum. Therefore adding the bispectrum data could help in breaking some degeneracies, e.g., the one between the neutrino mass and modified gravity parameters.

From this discussion, it is clear that the CMB bispectrum will provide interesting bounds, competitive with those coming from ISW-galaxy measurements while only marginally better than the constraints from CMB lensing trispectrum data. In any case, combining the bispectrum data with other CMB data sets, will definitely help improve the bounds and break some degeneracies.

VII. CONCLUSIONS

High accuracy temperature maps of the CMB anisotropy from ongoing and future experiments will provide an unique opportunity to test non-Gaussianity. While some of the signal could be primordial, a clear non-Gaussian signal is expected from the correlation of lensing and the Integrated Sachs-Wolfe effect. This signal provides a new test of the cosmological scenario *per se*, and could further be used to test alternatives to the cosmological constant in the context of cosmic acceleration. In this paper we have considered three different parametrizations of modified gravity and investigated the improvement in constraining their parameters by including the signal in the bispectrum coming from lensing-ISW correlations. We have found that in the case when all the cosmological parameters are fixed, the bispectrum signal will be extremely useful providing a significant improvement in the constraints on modified theories of gravity. While the forecasted constraints have been obtained with the assumption of the cosmological concordance model as the fiducial one, we believe that our results have little dependence on this choice, since current data accepts only relatively small deviations from the standard picture.

Moreover, we have assumed an ideal experiment, cosmic variance limited up to $\ell \sim 1000$ with a sky fraction $f_{\rm sky} = 0.65$. This is a good approximation for an experiment such as Planck, which is expected to be cosmic variance limited up to $\ell \sim 1500$. This amounts to neglecting systematics in the detectors noise, experimental beams and foreground removal that are present in the real world and would, to some degree, weaken the constraints presented in this paper. However, one could for instance include in the analysis polarization data, (that we have not considered here), to compensate for the loss of constraining power due to systematics.

Finally, while the L-ISW bispectrum signal will be presumably detected by the Planck satellite mission at about four standard deviations, the CMB lensing signal will be detected at much higher statistical significance and could also provide useful constraints on modified gravity theories (see e.g., Ref. [54]). However, CMB lensing is not directly sensitive to time variations in the gravitational potentials, which instead enters directly in the L-ISW signal. Measurements of the ISW signal through correlations of CMB maps with galaxy surveys already provide interesting constraints on the models presented here [26], however only a marginal future improvement in this measurement is expected. As we have shown, the constraints coming from observations of the L-ISW bispectrum, being sensitive to both the spatial gradient and the time variation of the Weyl potential, will be complementary to these other observations, improving CMB bounds on modified theories of gravity.

ACKNOWLEDGMENTS

The work of E. D. V., A. M., and V. S. was supported by the PRIN-INAF grant "Astronomy probes fundamental physics," by the Italian Space Agency through the ASI Contract No. Euclid-IC (I/031/10/0). A. S. is supported by NSF Grant No. AST-0708501.

[1] A. A. Starobinsky, Phys. Lett. **91B**, 99 (1980).
[2] S. Capozziello, S. Carloni, and A. Troisi, Recent Res. Dev. Astron. Astrophys. **1**, 625 (2003).
[3] S. M. Carroll, V. Duvvuri, M. Trodden, and M. S. Turner, Phys. Rev. D **70**, 043528 (2004).
[4] A. A. Starobinsky, JETP Lett. **86**, 157 (2007).
[5] G. Cognola, E. Elizalde, S. Nojiri, S. D. Odintsov, L. Sebastiani, and S. Zerbini, Phys. Rev. D **77** 046009 (2008).
[6] G. Esposito-Farese and D. Polarski, Phys. Rev. D **63**, 063504 (2001).

[7] N. Bartolo and M. Pietroni, Phys. Rev. D **61**, 023518 (1999).
[8] E. Elizalde, S. Nojiri, and S. D. Odintsov, Phys. Rev. D **70**, 043539 (2004).
[9] T. Chiba, Phys. Lett. B **575**, 1 (2003).
[10] G. R. Dvali, G. Gabadadze, and M. Porrati, Phys. Lett. B **485**, 208 (2000).
[11] C. Deffayet, Phys. Lett. B **502**, 199 (2001).
[12] G. Dvali, S. Hofmann, and J. Khoury, Phys. Rev. D **76**, 084006 (2007).
[13] Y.-S. Song, W. Hu, and I. Sawicki, Phys. Rev. D **75**, 044004 (2007).
[14] R. Bean, D. Bernat, L. Pogosian, A. Silvestri, and M. Trodden, Phys. Rev. D **75**, 064020 (2007).
[15] L. Pogosian and A. Silvestri, Phys. Rev. D **77**, 023503 (2008).
[16] S. Tsujikawa, Phys. Rev. D **77**, 023507 (2008).
[17] G.-B. Zhao, L. Pogosian, A. Silvestri, and J. Zylberberg, Phys. Rev. D **79**, 083513 (2009).
[18] A. Lue, R. Scoccimarro, and G. Starkman, Phys. Rev. D **69**, 044005 (2004).
[19] K. Koyama and R. Maartens, J. Cosmol. Astropart. Phys. 01 (2006) 016.
[20] Y.-S. Song, I. Sawicki, and W. Hu, Phys. Rev. D **75**, 064003 (2007).
[21] Y.-S. Song, Phys. Rev. D **77**, 124031 (2008).
[22] A. Cardoso, K. Koyama, S. S. Seahra, and F. P. Silva, Phys. Rev. D **77**, 083512 (2008).
[23] T. Giannantonio, Y.-S. Song, and K. Koyama, Phys. Rev. D **78**, 044017 (2008).
[24] R. Caldwell, A. Cooray, and A. Melchiorri, Phys. Rev. D **76**, 023507 (2007).
[25] S. F. Daniel, R. R. Caldwell, A. Cooray, and A. Melchiorri, Phys. Rev. D **77**, 103513 (2008).
[26] T. Giannantonio, M. Martinelli, A. Silvestri, and A. Melchiorri, J. Cosmol. Astropart. Phys. 04 (2010) 030.
[27] M. Martinelli, E. Calabrese, F. De Bernardis, A. Melchiorri, L. Pagano, and R. Scaramella, Phys. Rev. D **83**, 023012 (2011).
[28] S. F. Daniel, E. V. Linder, T. L. Smith, R. R. Caldwell, A. Cooray, A. Leauthaud, and L. Lombriser, Phys. Rev. D **81**, 123508 (2010).
[29] E. Komatsu, N. Afshordi, N. Bartolo, D. Baumann, J. R. Bond, E. I. Buchbinder, C. T. Byrnes, and X. Chen *et al.*, arXiv:0902.4759.
[30] N. Bartolo, E. Komatsu, S. Matarrese, and A. Riotto, Phys. Rep. **402**, 103 (2004).
[31] S. Das, B. D. Sherwin, P. Aguirre, J. W. Appel, J. R. Bond, C. S. Carvalho, M. J. Devlin, and J. Dunkley *et al.*, Phys. Rev. Lett. **107**, 021301 (2011).
[32] A. van Engelen, R. Keisler, O. Zahn, K. A. Aird, B. A. Benson, L. E. Bleem, J. E. Carlstrom, and C. L. Chang *et al.*, arXiv:1202.0546.
[33] S. Mollerach, A. Gangui, F. Lucchin, and S. Matarrese, Astrophys. J. **453**, 1 (1995).
[34] S. Mollerach and S. Matarrese, Phys. Rev. D **56**, 4494 (1997).
[35] D. M. Goldberg and D. N. Spergel, Phys. Rev. D **59**, 103002 (1999).
[36] L. Verde and D. N. Spergel, Phys. Rev. D **65**, 043007 (2002).
[37] B. Gold, Phys. Rev. D **71**, 063522 (2005).
[38] F. Giovi, C. Baccigalupi, and F. Perrotta, Phys. Rev. D **71**, 103009 (2005).
[39] K. M. Smith and M. Zaldarriaga, Mon. Not. Roy. Astron. Soc. **417**, 2 (2011).
[40] A. Mangilli and L. Verde, Phys. Rev. D **80**, 123007 (2009).
[41] P. Serra and A. Cooray, Phys. Rev. D **77**, 107605 (2008).
[42] D. Hanson, K. M. Smith, A. Challinor, and M. Liguori, Phys. Rev. D **80**, 083004 (2009).
[43] A. Lewis, A. Challinor, and D. Hanson, J. Cosmol. Astropart. Phys. 03 (2011) 018.
[44] E. V. Linder and R. N. Cahn, Astropart. Phys. **28**, 481 (2007).
[45] E. Bertschinger and P. Zukin, Phys. Rev. D **78**, 024015 (2008).
[46] Y.-S. Song, W. Hu, and I. Sawicki, Phys. Rev. D **75**, 044004 (2007).
[47] W. Hu and I. Sawicki, Phys. Rev. D **76**, 064004 (2007).
[48] R. K. Sachs and A. M. Wolfe, Astrophys. J. **147**, 73 (1967).
[49] http://www.sfu.ca/~aha25/MGCAMB.html
[50] E. Komatsu *et al.* (WMAP Collaboration), Astrophys. J. Suppl. Ser. **192**, 18 (2011).
[51] E. Calabrese, J. Smidt, A. Amblard, A. Cooray, A. Melchiorri, P. Serra, A. Heavens, and D. Munshi, Phys. Rev. D **81**, 043529 (2010).
[52] Y.-S. Song, H. Peiris, and W. Hu, Phys. Rev. D **76**, 063517 (2007).
[53] G.-B. Zhao, T. Giannantonio, L. Pogosian, A. Silvestri, D. J. Bacon, K. Koyama, R. C. Nichol, and Y. -S. Song, Phys. Rev. D **81**, 103510 (2010).
[54] E. Calabrese, A. Cooray, M. Martinelli, A. Melchiorri, L. Pagano, A. Slosar, and G. F. Smoot, Phys. Rev. D **80**, 103516 (2009).